AD 414881

QUARTERLY PROGRESS REPORT
SPUR POWER SYSTEM
CONTRACT AF33(657)-8954
FOR PERIOD ENDING MARCH 31, 1963
PROJECT NUMBER 3145
TASK NUMBER 314511

SY-5396-R4 April 15, 1963

GARRETT

AIRESEARCH MANUFACTURING COMPANY
A DIVISION OF THE GARRETT CORPORATION
PHOENIX, ARIZONA

QUARTERLY PROGRESS REPORT
SPUR POWER SYSTEM
CONTRACT AF33(657)-8954
FOR PERIOD ENDING MARCH 31, 1963
PROJECT NUMBER 3145
TASK NUMBER 314511

SY-5396-R4 April 15, 1963

Prepared by F. B. Wallace/R. W. Heldenbrand

Initial Issue
Approved by W. N. Blatt
W. N. Blatt, Supvr Pwr Turb Group

R. D. Gruntz
R. D. Gruntz, Supvr SPUR Conv Loop

J. H. Dannan III
J. H. Dannan, SPUR Proj Engr

Lyle D. Six
L. D. Six, Chief, Advanced Power Generation

THE GARRETT CORPORATION
AiResearch Manufacturing Division
Phoenix, Arizona

REPORT NO. SY-5396-R4

TOTAL PAGES 72

NOTICE

To expedite dissemination of technical information this report is being made available prior to approval or review by ASD. Consequently this report does not necessarily represent the views of ASD or the USAF. Comments and/or suggestions regarding the information contained in this report are welcomed. Comments and/or suggestions should be directed to ASD (WWRMFP-1), Wright-Patterson Air Force Base, Ohio.

ATTACHMENTS:

REV	BY	APPROVED	DATE	PAGES AND/OR PARAGRAPHS AFFECTED

ABSTRACT

This report, submitted by the AiResearch Manufacturing Company of Arizona, Phoenix, Arizona, a division of The Garrett Corporation, describes work accomplished in the period from January 1, 1963 to March 31, 1963, under Phase II of the SPUR Program, in accordance with United States Air Force Contract AF33(657)-8954.

The Phase II contract provides for continued analytical and experimental studies in support of the Space Power Unit, Reactor (SPUR) Program. Progress is reported for a total of 32 tasks.

In addition to a discussion of the work accomplished by AiResearch, the prime contractor, this report contains a discussion of the work accomplished by Aerojet-General Nucleonics (reactor system), Westinghouse Electric Corporation (electrical generator), General Electric Company (alternate turbogenerator), and Battelle Memorial Institute (material support). The program progress on each of these tasks is discussed in Section II.

TABLE OF CONTENTS

TABLE OF CONTENTS (Cont'd)

TABLE OF CONTENTS (Cont'd)

LIST OF FIGURES

LIST OF FIGURES (Cont'd)

LIST OF TABLES

THE GARRETT CORPORATION
AiResearch Manufacturing Division
Phoenix, Arizona

QUARTERLY PROGRESS REPORT
SPUR POWER SYSTEM
CONTRACT AF33(657)-8954
FOR PERIOD ENDING MARCH 31, 1963
PROJECT NUMBER 3145
TASK NUMBER 314511

I INTRODUCTION

The Space Power Unit, Reactor (SPUR) Program was initiated by the United States Air Force, in cooperation with the Atomic Energy Commission, in May of 1960. The ultimate objective of the SPUR Program is to develop a nuclear-dynamic space power system capable of supplying 300 kilowatts or more of electrical power, with a design life of 10,000 hours.

The power system will consist of a nuclear reactor as a heat source, the mechanical means of converting thermal energy to electrical energy, a radiator for rejection of waste heat, controls, and all other necessary auxiliary equipment. The thermodynamic conversion system will be a closed-cycle dynamic system, capable of operating unattended under the specified conditions. An electromagnetic-type generator is used to produce the electric power.

A description of the SPUR system and its components is included in the SPUR Phase I Final Report, ASD Technical Report ASD TR 61-656.

The objectives ot the Phase II Program are to continue portions of the study and experimental program initiated under Contracts AF33(616)-7379 and AF33(616)-8322 and to investigate several additional areas through analysis and experiment. The major technical work areas are as follows:

Materials testing, including creep-rupture and fatigue evaluation of Mo + 1/2 w/o Ti and Cb + 1 w/o Zr.

Mass-transfer tests of Cb + 1 w/o Zr with two-phase potassium flow.

Fabrication studies, including evaluation of methods for joining refractory metals in heat exchangers and in the radiator

Liquid-potassium bearing tests and analysis

Turbine performance test-rig design

Turbine material-erosion tests

Complete generator and generator test-rig designs

Continued development of the generator stator seal and insulation system.

Design and fabrication of a 50-kw liquid-metal-cooled, model generator.

Boiling potassium heat-transfer tests.

Study of flow stability and heat-transfer flow processes, including development tests on a separator.

Design of stainless steel heat-transfer components and a heat-transfer test loop.

Steady-state and load-change control analysis and a start-up control analysis and simulation test.

Reactor-loop pump analysis and bearing test, and loop dynamic simulation.

Reactor-loop control analog simulation.

II TECHNICAL DISCUSSION

The following paragraphs include a discussion of the program progress through March 31, 1963.

The various tasks are designated by the paragraph number from Contract AF33(657)-8954, and are discussed on subsequent pages.

Tasks accomplished under subcontract are listed below. The remaining tasks were accomplished by AiResearch, the prime contractor.

Battelle Memorial Institute: Four of the materials development tasks, pages 5 through 15.

Westinghouse Electric Corporation: General Development, pages 39 through 48.

General Electric: Alternate Turbogenerator, pages 49 through 53.

Aerojet-General Nucleonics: Reactor Loop, pages 63 through 65.

A. Materials Development

1. Creep-Rupture of Mo + 1/2 w/o Ti in Potassium Vapor at 2000°F - Task 2.2.2.1

Tests to extend the creep-rupture data for Mo + 1/2 w/o Ti in potassium vapor to 2000°F were continued. Tubular specimens, with potassium vapor sealed inside, were tested in conventional vacuum-creep apparatus. The tests were conducted in a vacuum of less than 0.5 x 10^{-8} torr.

Ten tests are involved in this task; four were completed and two more initiated during the previous quarter. Table I summarizes the conditions and results of all tests to date. Deformation-time curves for tests completed during this quarter are shown in Figures 1 and 2. Figure 3 shows minimum creep rates for the various stresses at 1800°F and 2000°F; Figures 4 and 5 present design curves for stress-relieved Mo + 1/2 w/o Ti at the two temperatures, respectively.

With the exceptions of Test No. 6, which was interrupted twice by furnace failures, and Test No. 7, in which the specimen ruptured near a fillet, all completed tests proceeded normally and data are considered reliable. Tests No. 6 and No. 7 were intended as comparison tests with Test No. 5, which also was interrupted by a furnace failure. As indicated by the time-deformation curve for Test No. 5 on Figure 1, however, the interruption, which occurred 190 hours after start of the test, did not appear to influence the creep rate significantly. Also, the minimum creep rates for both Tests No. 5 and No. 7 are identical. The fact that Test No. 6 (helium-filled specimen) appeared to proceed normally until its second interruption and that its minimum creep was slightly greater than for Tests No. 6 and No. 7 appears to support the general conclusion that a potassium vapor environment is not detrimental to the creep properties of arc-case, hot-rolled, stress-relieved Mo + 1/2 w/o Ti at 2000°F.

Test No. 9, now in progress, will complete this series.

TABLE I

CREEP-RUPTURE TESTS ON Mo + 1/2 w/o Ti

	1	2	3	4	5	6	7	8	9	10
Specimen type	Hollow	Solid bar	Hollow	Hollow	Hollow	Hollow	Hollow	Hollow	Hollow	Hollow
Stress, psi	35,000	35,000	35,000	48,000	25,000	25,000	25,000	50,000	55,000	60,000
Temperature, °F	2000	2000	2000	2000	2000	2000	2000	1800	1800	1800
Internal environment	He	-	K	K	K	He	K	K	K	K
Estimated time to rupture, hr	100	100	100	10	700	700	700	350	100	30
Actual time to rupture, hr	101.1	116.2	140.6	9.2	496.8	310[b]	488.3[c]	266.3	(d)	30.9
Elongation at fracture, percent	11.1	12.7	15.0	16.0	12.0	12.3	4.3	12.0	-	9.9
Reduction of area at fracture, percent	90 +	88.6	90 +	90 +	90 +	90 +	90 +	90 +	-	90 +
Minimum creep rate, percent/hr	0.017	0.016	0.016	0.36	0.0011	0.0015	0.001	0.010	-	0.103
Specimen appearance after test	Bright	Bright	Bright	Bright	Bright	Bright	Bright	Bright	-	Bright

(a) Cannot make precise reduction-of-area measurements on hollow specimen fractures.

(b) This rupture time is not reliable because the rig furnace failed twice during the test; and after the second failure (at 190 hrs), the creep rate increased immediately.

(c) Rupture occurred near the fillet.

(d) Test in progress.

FORM P 8787A-1

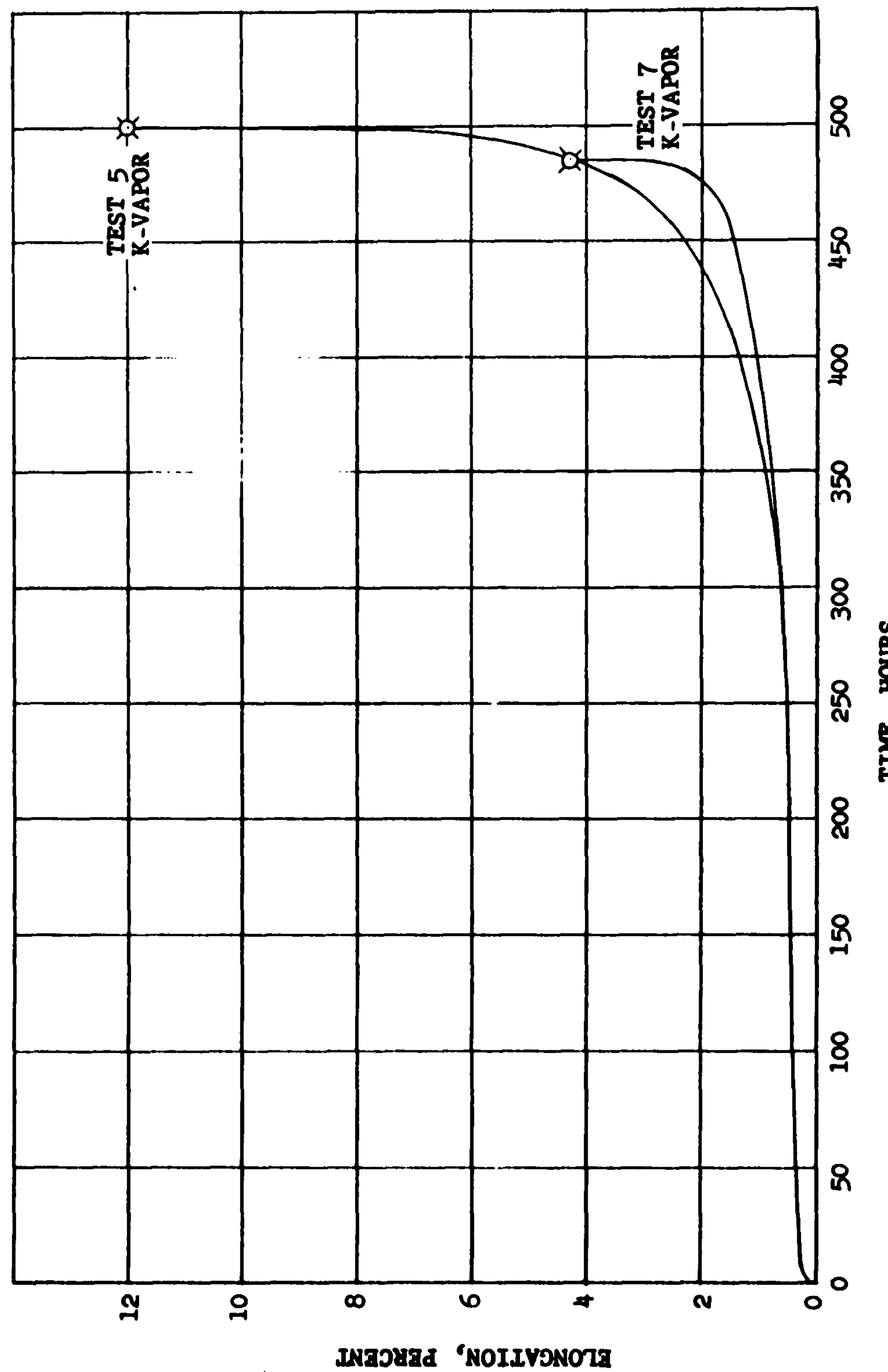

FIGURE 1. DEFORMATION-TIME CURVES FOR 2000°F
Mo + 1/2 w/o Ti AT 25,000 PSI TENSILE STRESS
UNDER HELIUM AND POTASSIUM VAPOR ENVIRONMENTS

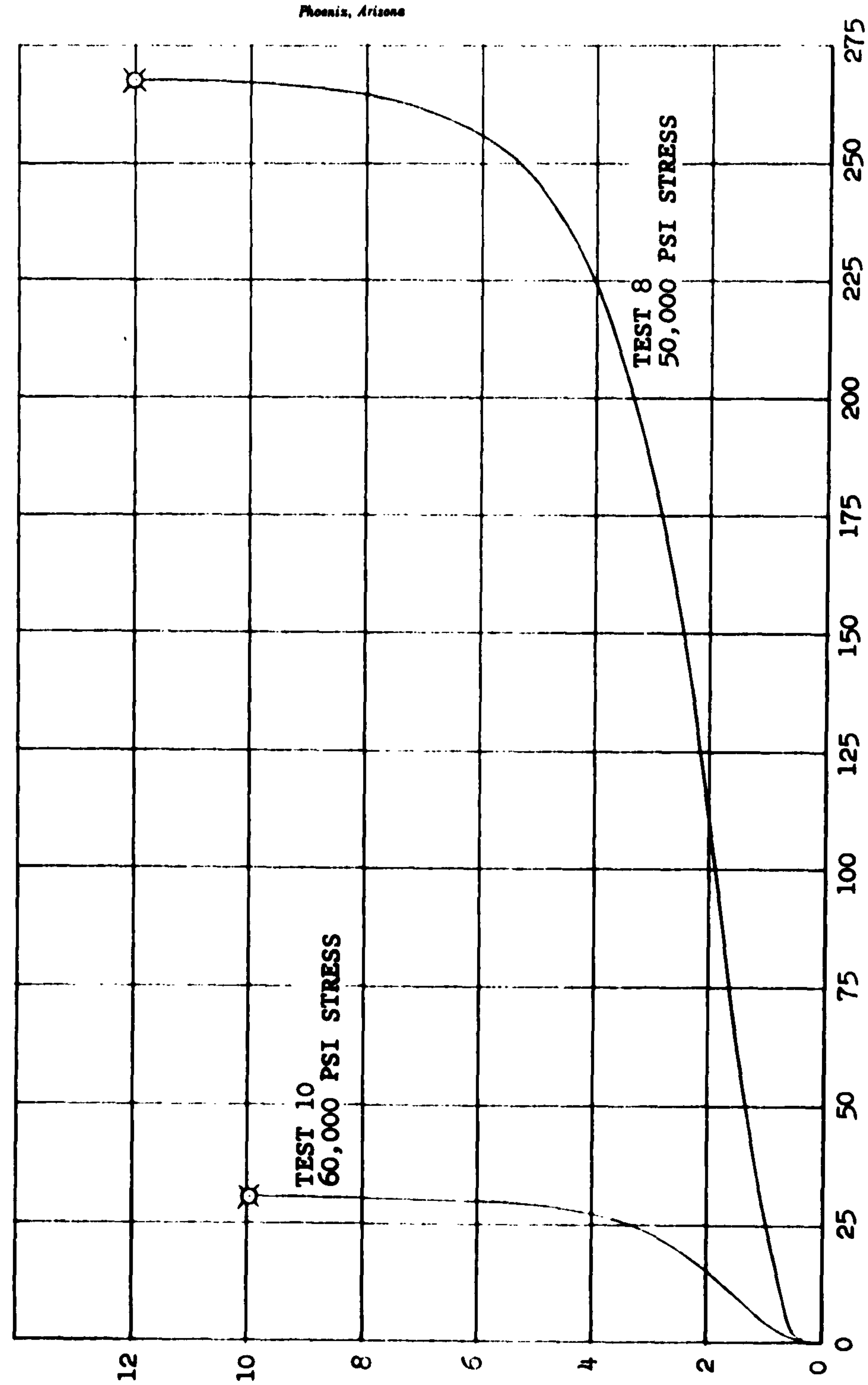

FIGURE 2. DEFORMATION-TIME CURVES FOR 1800°F Mo + 1/2 w/o Ti IN POTASSIUM VAPOR

FORM P 8787A-1

THE GARRETT CORPORATION
AiResearch Manufacturing Division
Phoenix, Arizona

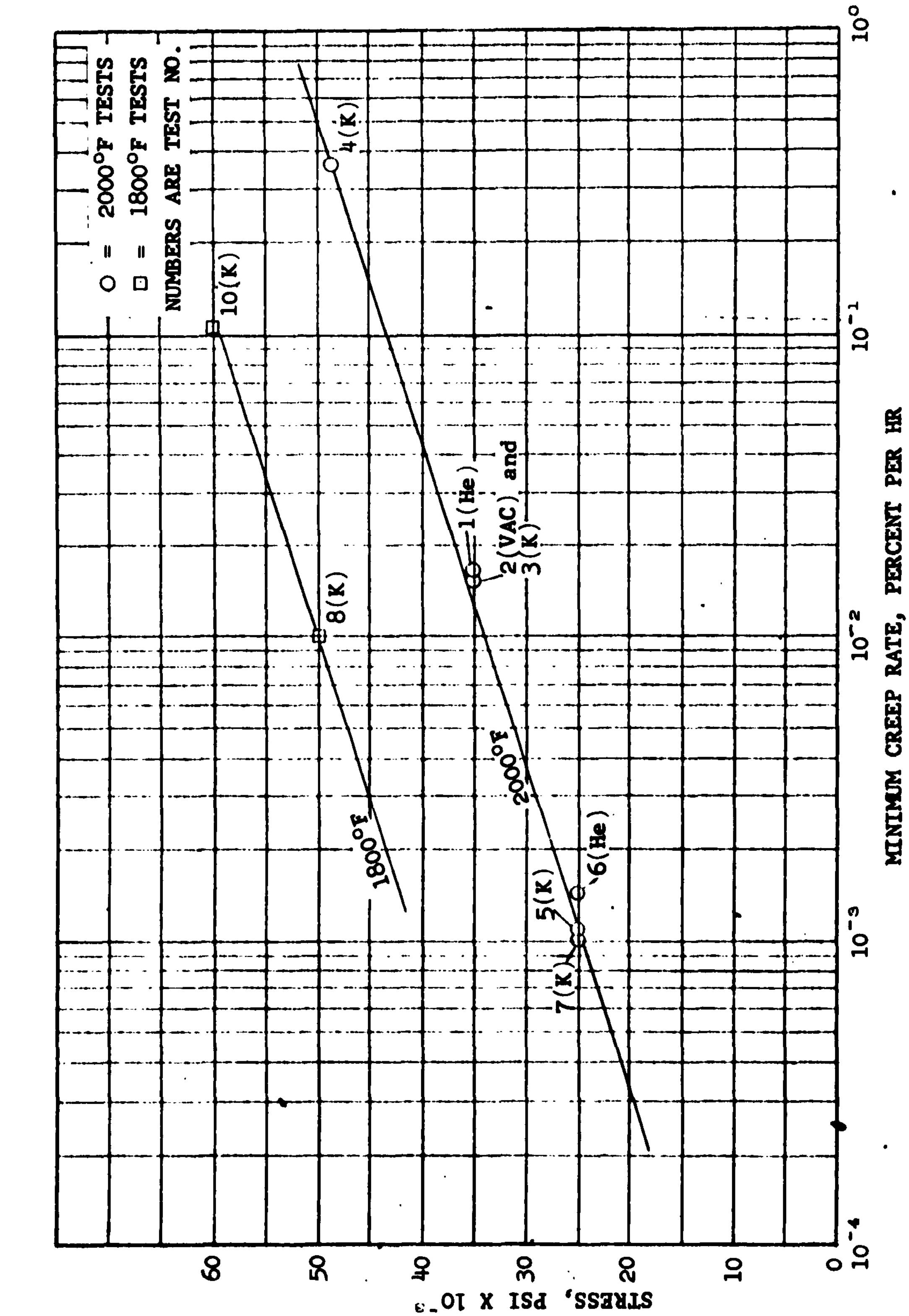

FIGURE 3. STRESS VS MINIMUM CREEP RATE FOR Mo + 1/2 w/o Ti IN HELIUM AND POTASSIUM VAPOR AT 1800°F AND 2000°F

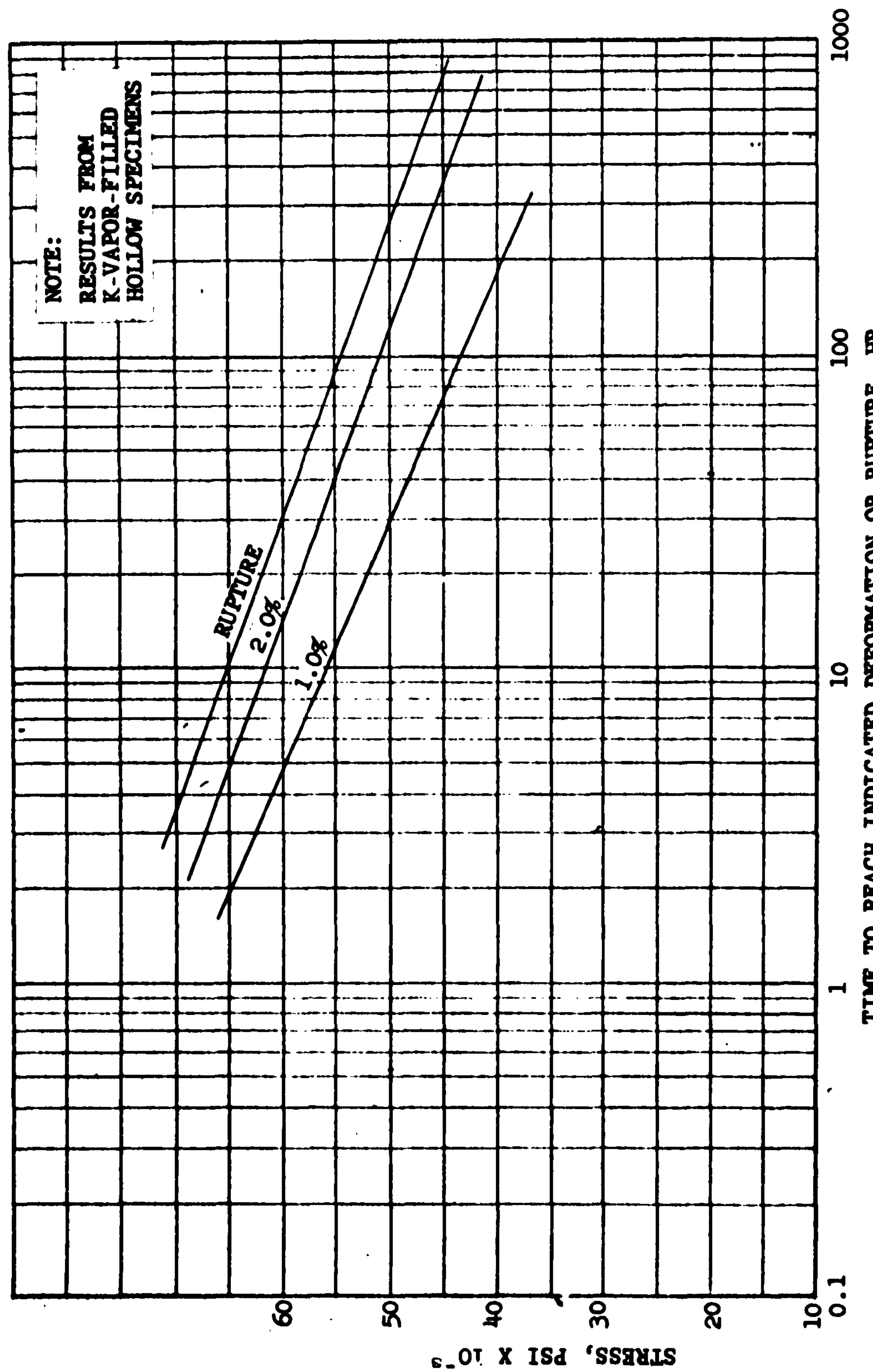

FIGURE 4. DESIGN CURVES FOR STRESS-RELIEVED Mo + 1/2 w/o Ti AT 1800°F

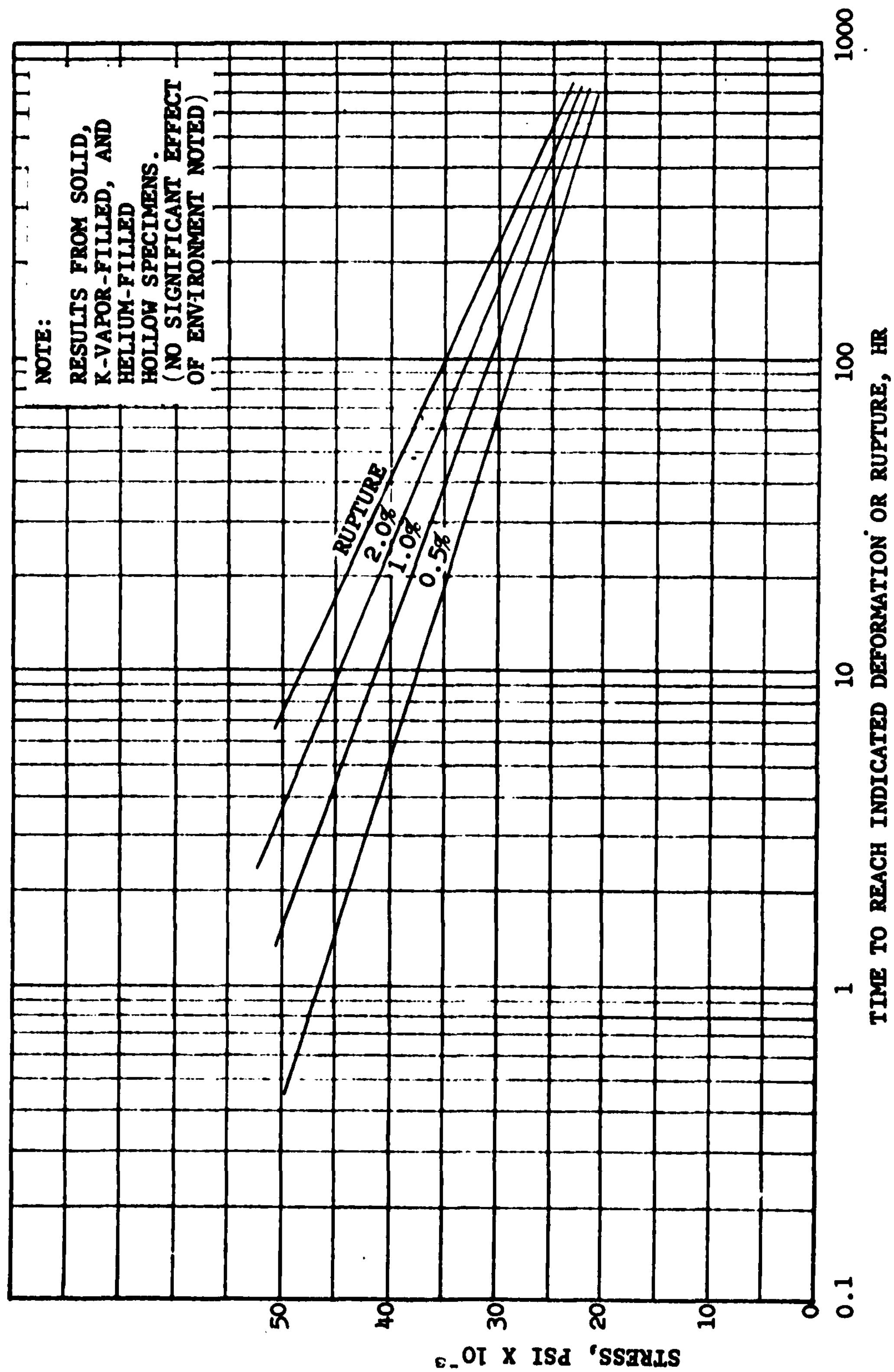

FIGURE 5. DESIGN CURVES FOR STRESS-RELIEVED Mo + 1/2 w/o Ti AT 2000°F

2. Fatigue of Mo + 1/2 w/o Ti in Potassium Vapor at 2000°F - Task 2.2.2.2

During the past quarter, initial fatigue tests were run in the apparatus adapted to an Ivy Dynamic Creep Tester for this task. A description of the apparatus and the adaptation were given in the Phase II Annual Technical Summary Report (Confidential), SY-5457-R, dated January 31, 1963. The objective is to obtain design data on the behavior of Mo + 1/2 w/o Ti under the influence of cyclic stresses in an environment of potassium vapor at temperatures of 1500°F and 2000°F. Comparison tests in the same apparatus with a helium or vacuum atmosphere will be run. Four S-N curves (two at each temperature and environment) are to be generated.

In the first test, a 1500°F helium-filled specimen was run out to 10^8 cycles at 35,000 psi maximum stress without fracture or recordable creep. The maximum stress was then increased to 50,000 psi and the test continued. The purpose of the additional testing was to gather general information on suitable stress ranges for future tests. The specimen failed after 525,000 cycles and approximately 0.002 inch creep at the higher stress level. The apparatus performed satisfactorily during the test, and the specimen fatigue fracture was typical.

A second test of a 1500°F helium-filled specimen is in progress. To date, it has undergone a maximum stress of 47,500 psi for over 6×10^7 cycles.

Apparatus for a second machine was fabricated and is being assembled. The 2000°F tests will be initiated in this rig as soon as possible.

3. Cantilever Bending Fatigue of Cb + 1 w/o Zr in Liquid Potassium and Liquid Lithium - Task 2.2.2.3

The tests in 800°F potassium were completed in January 1963; complete results were given in the Phase II Annual Technical Summary Report (Confidential), SY-5457-R, January 31, 1963. On the basis of the data generated, the alloy would be expected to sustain the following reversed-bending stresses for the indicated number of cycles in 800°F potassium:

Range of Maximum Bending Stress, psi	Lifetime, Cycles
35,000 to 39,000	10^5
29,500 to 31,500	10^6
27,000 to 27,500	10^7

The apparatus used for the potassium tests was modified for the 1600°F lithium tests, and two tests were completed during the past quarter. In the first of these tests, a specimen was subjected to 30,000 psi maximum bending stress (based on a modulus of 12 x 10^6) and fractured after 10,000 cycles. In the second test at 25,000 psi maximum bending stress, the specimen failed between 21,000 and 52,000 cycles. The exact time of failure could not be determined because the sensing-rod movement (approximately 0.0003 inch) was not sufficient to shut off the machine at fracture. However, results are expected to be of some value in establishing the S-N curve. The rig was modified to improve the sensitivity of the sensing mechanism.

Up to eight additional tests will be performed.

4. Creep Rupture of SAE 4340 Steel in Potassium Vapor at 1000°F

The experimental investigations to evaluate the creep-rupture properties of SAE 4340 steel have been completed. A comparison of the results of the tests of SAE 4340 steel in a potassium vapor environment with the results of comparable tests in an air environment indicates that potassium vapor has little or no influence on the creep-rupture properties of this alloy. A topical report of the test results has been prepared, and copies were furnished to the Aeronautical Systems Division for review and approval as a Technical Documentary Report.

5. Mass Transfer Tests with Two-Phase Flow - Task 2.2.2.4

During the previous report period, testing of the tantalum heaters was accomplished, showing satisfactory operation in all respects except that some contamination of the tantalum heaters occurred due to outgassing of the boron nitride insulation. (The boron nitride had been baked out at 1800°F in air.) Subsequently, bakeout at 1800°F in a 10-micron vacuum was found to reduce contamination, although some contamination was noted. A 15-hour bakeout of the boron nitride was then accomplished at 2200°F and a pressure of 10^{-6} torr. This bakeout procedure was found to eliminate the contamination of the tantalum, and this procedure has now been adopted as the bakeout procedure for the test loop insulators.

The loop was assembled using an inert-gas welding procedure within a gas bag (shown on Figure 6). Analysis of weld coupons showed no significant oxygen or nitrogen pickup in the welds. The assembled loop is shown on Figure 7.

A leak check and pressure checks of the chamber and purification system were completed. A second system leak check is scheduled during April.

A pressure-relief valve has been designed for the chamber to allow release of any overpressure while the loop is in operation. (This condition could possibly occur if a double failure of the argon pressure controls occurred.)

The tantalum heaters and radiator shield have been welded to the loop, as shown in Figure 7, also using the gas-bag, inert-atmosphere welding procedure. Thermocouples have also been installed on loop heaters.

LAYOUT OF Cb + 1 w/o Zr TEST LOOP
FOR INERT GAS WELDING

INERT GAS WELDING OF Cb + 1 w/o Zr
TEST LOOP IN GAS BAG
FIGURE 6

ASSEMBLED Cb + 1 w/o Zr TEST LOOP
AFTER TANTALUM WRAP

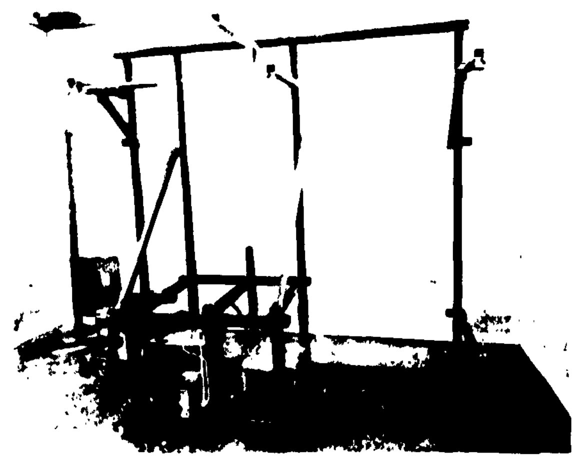

ASSEMBLED LOOP WITH HEATERS INSTALLED

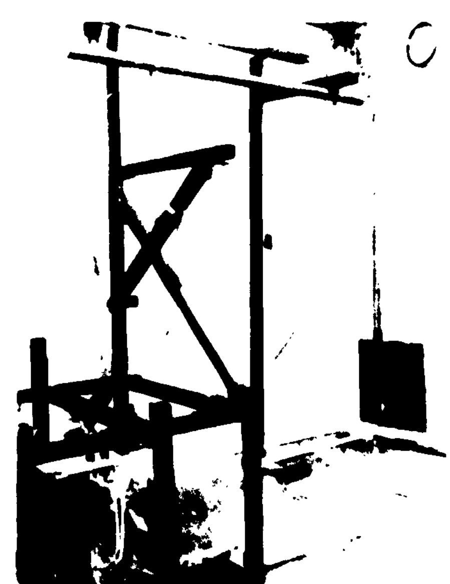

TWO-PHASE POTASSIUM CORROSION TEST LOOP

FIGURE 7

6. Liquid-Potassium Mass-Transfer Tests - Task 2.2.2.5

As reported in the Phase II Annual Technical Summary Report, SY-5457-R (Confidential), the preliminary design of the liquid-potassium mass transfer loop was completed. A schematic drawing of the loop was included in that report. This task is now complete.

7. Brazed Alloy Compatibility Tests

The metallograph of the braze samples exposed to potassium in standard capsules for 500 hours at 1500° and 2000°F has been completed. The metallograph, weight change measurements, and test conditions are shown in Table II. Table III tabulates the chemical analysis of those capsules which successfully completed the 500-hour test. No logical reason can be given to the increase of iron in capsule 9. The metallography does not indicate any reaction to support this iron pickup. The general conclusions which can be drawn from these tests are the following: (1) the braze samples show excessive base metal reaction indicating poor temperature control during the brazing operation, (2) as a result of poor temperature control, braze alloy wetability characteristics cannot be accurately ascertained, (3) some contamination occurred during the brazing operation, (4) pure titanium appears to be the most promising of the braze alloys tested for 1500°F and 2000°F liquid potassium compatibility, and (5) the 48 Ti - 48 Zr - 4 Be braze alloy appears promising for use at 1500°F in potassium environment. Typical photomicrographs of the braze specimens are shown in Figures 8 and 9.

TABLE II

RESULTS OF VARIOUS BRAZE ALLOYS ON COLUMBIUM - 1 ZIRCONIUM
TESTED IN LIQUID AND VAPOR POTASSIUM REFLUX CAPSULES
FOR 500 HOURS AT 1500°F AND 2000°F

Capsule Number	Specimen	Braze Alloy	Test Temp °F	Test Time	Weight Before Test grams	Weight After Test grams	Weight Difference grams	Weight Loss mg/cm²/hr	Visual Results	Metallographic Results
1	C	Pure nickel							Small fillets - braze flowed over one leg of "T" joint.	Severe cracking through the braze alloy with needle-like phases present.
	A vapor	Pure nickel	1500	500 hours	3.2871	3.2791	-0.0080	0.0017	Small fillets - no apparent attack. Metal surfaces look clean.	Braze alloy shows attack but not preferential to needle phase.
	B liquid	Pure nickel	1500	500 hours	3.2950	3.2928	-0.0022	0.0005	Small fillets - no apparent attack. Metal surfaces look clean.	Braze alloy shows attack but not preferential to needle phase.
2	C	Pure nickel							Fair size fillets - braze flowed over one leg of "T" joint.	Slight cracking through braze alloy with needle-like phase present.
	A vapor	Pure nickel	2000	Capsule failed during test	3.2522	3.2518	-0.0004	--	Basis metal surfaces show severe attack.	No conclusions due to capsule failure.
	B liquid	Pure nickel	2000		3.3584	--	--	--	--	No conclusions due to capsule failure.
3	C	Pure titanium							Poor braze coverage approximately 75 percent of joint brazed.	No internal braze cracks. Braze alloy shows single-phase characteristics.
	A vapor	Pure titanium	1500	500 hours	3.1051	3.1044	-0.0007	0.0001	Slight braze alloy attack.	No preferential braze alloy attack observed.
	B liquid	Pure titanium	1500	500 hours	3.2981	3.2981	None	<0.1 Mg	Slight braze metal attack. No braze alloy in joint.	No preferential braze alloy attack observed.
4	C	Pure titanium							Very poor braze alloy coverage in T joint.	Braze fillet size is very irregular with erosion of basis metal. No cracks present.
	A vapor	Pure titanium	2000	500 hours	3.1603	3.1593	-0.0010	0.0002	No apparent braze alloy or basis metal attack.	No braze alloy attack observed.
	B liquid	Pure titanium	2000	500 hours	3.3389	3.3386	-0.0003	0.00006	No apparent braze alloy or basis metal attack.	No braze alloy attack observed.
5	C	48 Ti-48 Zr-4 Be							Small braze fillets with apparent dark oxide scale on surface of braze and basis metal.	No cracks in braze alloy. Braze alloy to basis metal joints show little diffusion.
	A vapor	48 Ti-48 Zr-4 Be	1500	500 hours	4.2183	4.2120	-0.0063	0.0013	Severe edge attack on basis metal.	Apparent braze alloy surface attack. Braze shows increased diffusion into basis metal.
	B liquid	48 Ti-48 Zr-4 Be	1500	500 hours	3.8703	3.8692	-0.0011	0.0002	No apparent attack.	Apparent braze alloy surface attack. Braze shows increased diffusion into basis metal.
6	C	48 Ti-48 Zr-4 Be							Good fillets and joint coverage.	No cracks in braze alloy.
	A (vapor)	48 Ti-48 Zr-4 Be	2000	Capsule failed during test.	3.8937	3.8752	-0.0185	0.0039	Severe braze alloy attack (6B appears worse than 6A).	No conclusions due to capsule failure.
	B liquid	48 Ti-48 Zr-4 Be	2000		3.9013	4.0672	+0.1659	+0.035	Very severe braze alloy attack.	No conclusions due to capsule failure.

TABLE II (Continued)

Capsule Number	Specimen	Braze Alloy	Test Temp °F	Test Time	Weight Before Test grams	Weight After Test grams	Weight Difference grams	Weight Loss mg/cm²/hr	Visual Results	Metallographic Results
7	C	60 Zr-25 V-15 Cb							Good fillets and braze coverage. Dark oxide on braze alloy surface.	No cracks in braze alloy.
	A vapor	60 Zr-25 V-15 Cb	1500	500 hours	5.1138	5.1128	- 0.0010	0.0002	Good fillets and braze coverage. Dark oxide on braze alloy surface.	No apparent braze alloy attack.
	B liquid	60 Zr-25 V-15 Cb	1500	500 hours	5.0162	5.0155	- 0.0007	0.0001	Sample looks similar to A .	No apparent braze alloy attack.
8	C	60 Zr-25 V-15 Cb							Braze shows irregular flow with discolored oversize and small fillets.	No cracks in braze alloy. Good fillete
	A vapor	60 Zr-25 V-15 Cb	2000	Capsule failed during test	4.9682	5.0087	+ 0.0405	-0.00856	Apparent attack of base metal and braze.	No conclusions due to capsule failure.
	B liquid	60 Zr-25 V-15 Cb	2000		5.0825	5.0914	+ 0.0089	+0.00188	Severe and irregular attack of base metal adjacent to braze alloy.	No conclusions due to capsule failure.
9	C	58 Zr-27 Ti-15 Fe							Braze fillets are good with slight braze alloy discoloration.	No cracks in braze alloy. Braze alloy to basis metal shows only slight diffusion.
	A vapor	58 Zr-27 Ti-15 Fe	1500	500 hours	5.0842	5.0794	- 0.0048	0.0010	No apparent attack.	No apparent braze alloy attack. Braze alloy shows increased diffusion zone.
	B liquid	58 Zr-27 Ti-15 Fe	1500	500 hours	4.7518	4.7489	- 0.0029	0.0006	No apparent attack.	No apparent braze alloy attack. Braze alloy shows increased diffusion zone.
10	C	58 Zr-27 Ti-15 Fe							Good braze fillets with slight oxide discoloration	No cracks in braze alloy
	A vapor	58 Zr-27 Ti-15 Fe	2000	500 hours	5.1871	5.0613	- 0.1258	0.0266	Severe braze alloy attack.	Severe braze alloy attack.
	B liquid	58 Zr-27 Ti-15 Fe	2000	500 hours	4.9798	4.8951	- 0.0847	0.0177	Severe braze alloy attack.	Severe braze alloy attack.
11	C	63 Ti-27 Fe-10 Mo							Good braze alloy fillet size with severe braze alloy surface cracks	Surface and internal cracks or shrinkage observed. Braze alloy to basis metal shows slight diffusion.
	A vapor	63 Ti-27 Fe-10 Mo	1500	500 hours	4.8853	4.8835	- 0.0018	0.0004	No apparent attack.	No apparent braze alloy attack. Braze alloy shows increased diffusion zone.
	B liquid	63 Ti-27 Fe-10 Mo	1500	500 hours	5.0450	5.0456	+ 0.0006	0.0001	No apparent attack.	No apparent braze alloy attack. Braze alloy shows increased diffusion zone.
12	C	48 Zr-48 Ti-4 Be							Small braze alloy fillets with slight surface oxidation.	No braze alloy cracks. Braze alloy to basis metal shows slight diffusion.
	A vapor	48 Zr-48 Ti-4 Be	1500	500 hours	5.0183	5.0182	- 0.0001	0.00002	No apparent attack.	No apparent braze alloy attack.
	B liquid	48 Zr-48 Ti-4 Be	1500	500 hours	5.1917	5.1913	- 0.0004	0.00008	No apparent attack.	No apparent braze alloy attack.

TABLE III

BRAZE ALLOY CAPSULE
POTASSIUM CHEMICAL ANALYSES

Element	Cb	Ni	Ti	Zr	Be	Fe	Mo	V	O_2
Detection Limit	10	5	5	5	1	5	5	5	5
Capsule					ppm				
1	N	N							
3	500		N						
4	N		N						
5	20		N	N	N				
7	100			N				N	
9	N		<10	N		100			
10	N		<10	N		<10			
11	N		<10			<10	N		
12	N		<10	N	N				
Fill Sample	N		<10	N	N	<10	N	N	34

NOTES: N = none detected
<10 = above detection limit, but less than 10 ppm

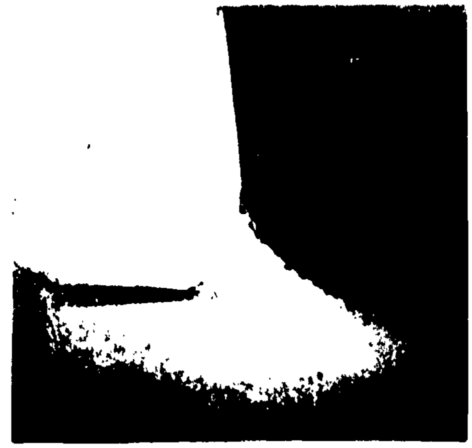

AS BRAZED

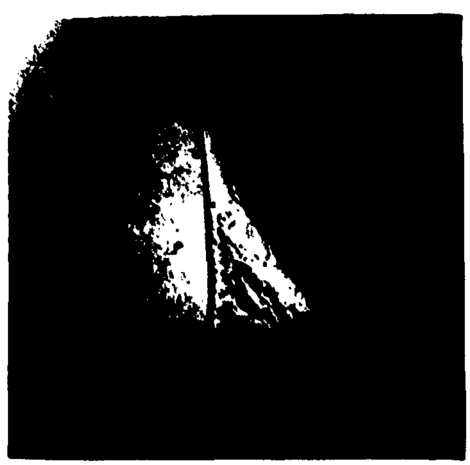

AFTER EXPOSURE TO LIQUID POTASSIUM VAPOR AT 1500°F FOR 500 HOURS

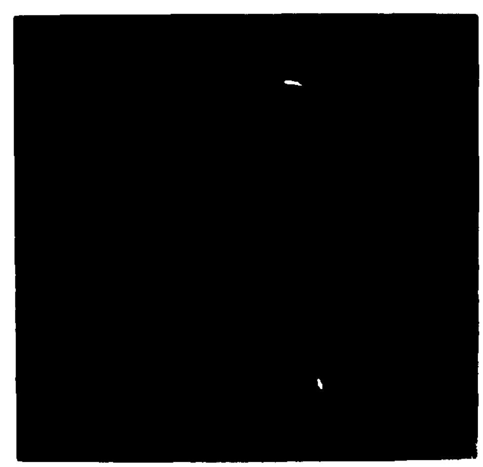

AFTER EXPOSURE TO LIQUID POTASSIUM AT 1500°F FOR 500 HOURS

MAGNIFICATION: 48X

PHOTOMICROGRAPHS OF COLUMBIUM - 1 W/O ZIRCONIUM ELECTRON BEAM BRAZED WITH 60 ZIRCONIUM - 25 VANADIUM - 15 COLUMBIUM BRAZE ALLOY AND TESTED IN A LIQUID POTASSIUM REFLUX CAPSULE AT 1500°F FOR 500 HOURS

FIGURE 8

AS BRAZED

AFTER EXPOSURE TO LIQUID
POTASSIUM AT 1500°F
FOR 500 HOURS

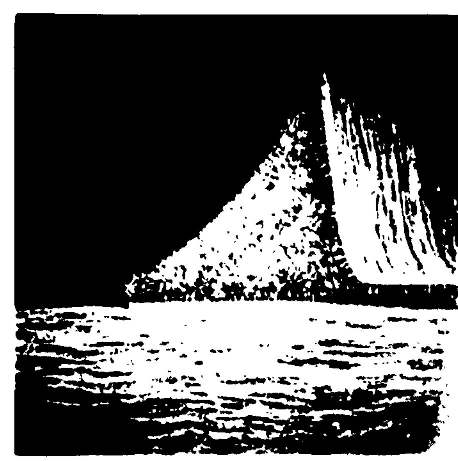

AFTER EXPOSURE TO LIQUID
POTASSIUM VAPOR AT 1500°F
FOR 500 HOURS

MAGNIFICATION: 48X

PHOTOMICROGRAPHS OF COLUMBIUM - 1 W/O ZIRCONIUM
ELECTRON BEAM BRAZED WITH 63 TITANIUM -
27 IRON - 10 MOLYBDENUM BRAZE ALLOY
AND TESTED IN A LIQUID POTASSIUM REFLUX CAPSULE
AT 1500°F FOR 500 HOURS

ETCHANT: H_2O 10cc
HNO_3 5cc
HF 3cc
H_2SO_4 2cc

FIGURE 9

8. Fabrication Studies - Task 2.2.2.7

The objective of this task was to evaluate promising methods of fabricating typical SPUR heat-transfer components.

The requirements of this task under Phase II have been completed, and the results were reported in the Phase II Annual Technical Summary Report, SY-5457-R (Confidential). Under this task, studies of methods of fabricating refractory-metal radiator tube-to-fin joints and heat exchanger tube-to-header joints were conducted; a study of techniques required for testing tube-to-header joints was also conducted; and a preliminary design of a suitable test rig has been completed.

B. Test Techniques

1. High-Temperature Heater Evaluation - Task 2.2.3.1

The objectives of this task were completed during the previous report period, and the results were reported in the last Quarterly Progress Report (SY-5396-R3).

Two 20-kilowatt heater designs were selected as most promising: (1) a design using resistance heating in the wall and conduction to the liquid metal, and (2) a design using the resistance of the liquid metal itself to furnish the heating. A test program has also been outlined for these two designs which will fully evaluate the heaters and permit final design of the 5-megawatt heater.

C. Bearing Development

1. Bearing Tests - Task 2.2.4.1.1

Assembly of the loop, checkout, insulation, and instrumentation calibration were completed in February. The loop was operated for approximately 250 hours, including 7-1/2 minutes of bearing operation at 15,000 rpm. The loop operations were terminated when a failure of an electromagnetic pump occurred.

A teardown inspection of the loop showed that the following series of events had occurred:

(a) A potassium plug developed at the drain from the test bearing.

(b) Formation of this plug allowed potassium to be forced up, past the seal, into the middle chamber. The high-temperature potassium caused deterioration of the carbon seal.

(c) At a later time, the oil drain from the middle chamber became partially plugged and the chamber became filled with oil. This head of oil caused leakage past the carbon seal into the lower chamber, contaminating the potassium loop with a carbonaceous material.

(d) At this time, the electromagnetic pump failed through burnout of the pumping section. The pump was found to be dry, due to the carbonaceous plugs that were formed in the lines. This condition may have contributed to the pump failure; but since the vendor's specification (and experience) indicated no difficulty when run dry, the failure should not have occurred.

The bearing test loop is now being rebuilt with the following design changes:

(a) A new seal, of the backup design initiated several months earlier, will be installed. This seal is shown in Figure 10 , and in the drawing, Figure 11.

(b) An oil level warning device is being installed in the middle chamber, and an oil sump sight glass is being installed.

POTASSIUM-TO-ARGON-TO-OIL
BACKUP SEAL FOR BEARING TEST RIG

FIGURE 10

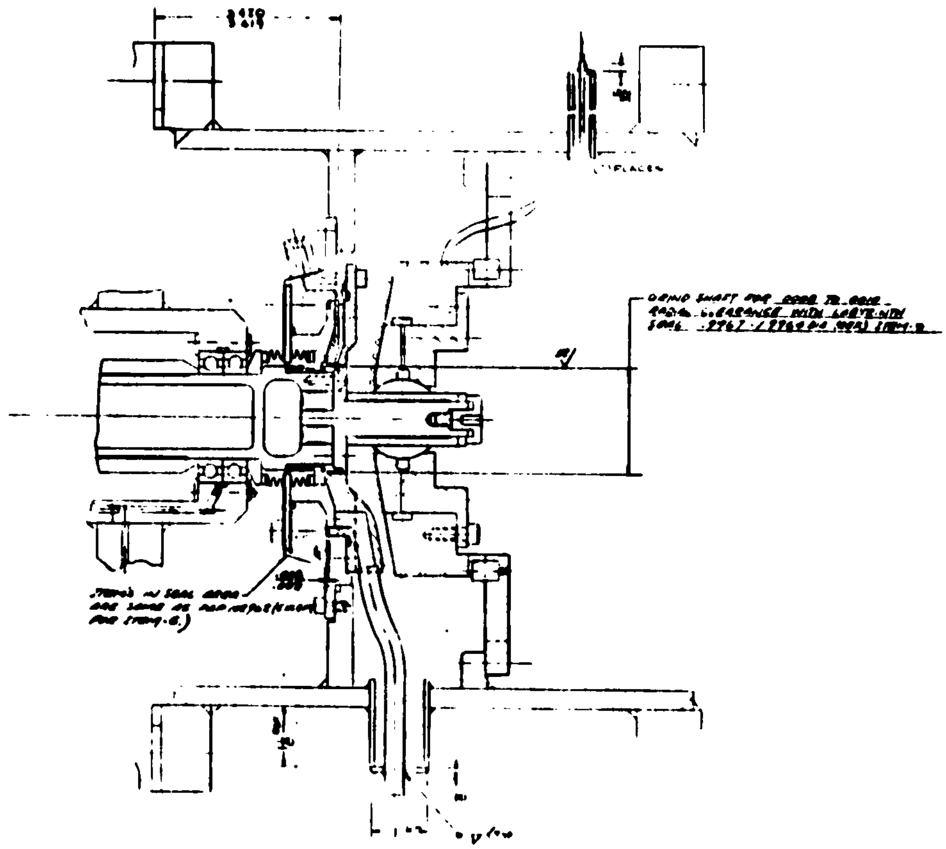

BEARING TEST LOOP BACKUP SEAL
FIGURE 11

(c) Heaters are being installed on the test bearing (see Figure 11). These heaters will eliminate the possibility of the test bearing section being cooled by the oil above the seal to a temperature below the potassium freezing point. In addition, the capacity of the heaters on the outside of the test section has been increased.

(d) The potassium line heaters have been modified for improved reliability, and warning lights have been installed on all heaters.

(e) The potassium lines are 3/8 inch in diameter, having been sized at the time the loop was intended to run rubidium, a substantially more expensive fluid. These tubes are being changed to 1/2-inch diameter wherever possible.

It is believed that these changes will eliminate recurrence of the difficulties experienced in this quarter. The most recent loop schematic is shown on Figure 12.

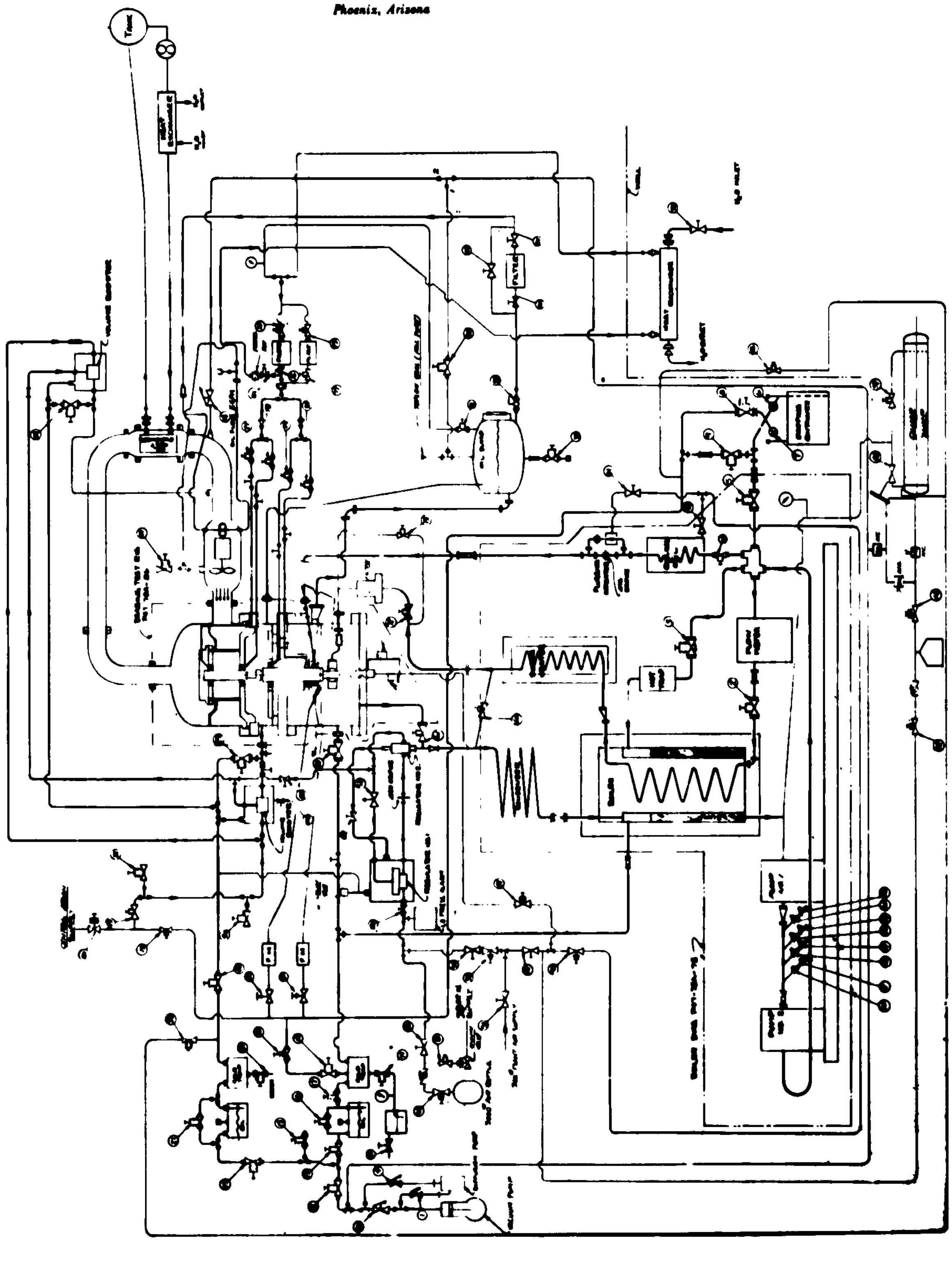

BEARING TEST LOOP SCHEMATIC
FIGURE 12

2. Bearing Analysis - Task 2.2.4.1.2

The analysis of journal bearing configurations for the SPUR turbogenerator has been completed, and a topical report of the results has been prepared. The topical report will be submitted to the Aeronautical Systems Division in April 1963 for review and approval as a Technical Documentary Report.

The bearing analysis used a computer program that solves the basic hydrodynamic equations, including consideration of fluid inertia forces in both the turbulent and laminar regimes. Solutions were obtained for a number of bearing configurations, using this program, with potassium as the lubricant. The classical laminar equations were also solved for identical bearing configurations, and comparisons between the two solutions were made. Several journal bearing mounting arrangements were considered, and a design was selected for initial testing.

D. Turbine Development

1. Turbine Performance Test Rig Design - Task 2.2.4.2.1

The design of the turbine performance test rig was completed, as reported in the last Quarterly Progress Report. The design of the test loop has been completed, and vendors for the major components have been selected. Design of the required instrumentation is also complete, and tooling for fabrication of the turbine test rig has been obtained.

The Phase II requirements for this task are now complete, and these activities will be continued under Phase III.

2. Turbine Material Erosion Tests - Task 2.2.4.2.2

A second potassium erosion test run was completed during this quarter. The materials tested were the same as those used in the previous test, namely Rene 41, stellite 6B, Mo + 1/2 w/o Ti and Mo + 1/2 w/o Ti + 0.08 w/o Zr (TZM). The duration of this test was, however, approximately twice that of the previous run (50.5 hours vs 26.6 hours). The erosion, as during the previous run, was not visible to the naked eye but was discernible as changes in specimen weight. Photomicrographs were made of the impact regions of the specimens and are shown in Figures 13 and 14. The first visible stages of erosion are indicated on the photomicrograph of the Rene 41 specimen as small pits. This is substantiated by the fact that the weight loss of the Rene 41 was approximately twice that of the other three materials. A summary of the test results is presented below.

TABLE IV

SECOND TURBINE MATERIALS EROSION TEST

Impact velocity:	212 ft per sec.
Liquid-potassium temperature:	1400°F
Potassium flow rate:	4.9 gpm
Weight loss of geometrically similar specimens:	
Rene 41:	0.0013 gram
Stellite 6B:	0.0007 gram
Mo + 1/2 w/o Ti:	0.0007 gram
Mo + 1/2 w/o Ti + 0.08 Zr:	0.0008 gram

Mo + 1/2 w/o Ti

TZM

TURBINE MATERIAL EROSION TESTS

FIGURE 13

RENE 41

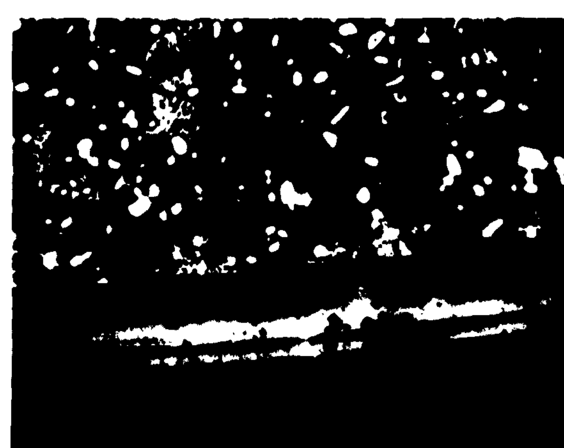

HS-6B

TURBINE MATERIAL EROSION TESTS

FIGURE 14

The results of the second erosion test again indicate that the erosion problem in potassium at elevated temperature is less severe than in water under similar conditions of impact velocity, stream diameter, and nozzle-to-specimen clearance. Furthermore, this second potassium test indicates that the erosion resistance of the molybdenum alloys used in the test is essentially the same as that of stellite 6B.

The testing program will continue in Phase III.

E. Generator Development

1. Generator Design - Task 2.2.4.3.1

The generator design was completed during the previous report period. The generator layout and electromechanical design drawings (Confidential drawings) were included in the Phase II Annual Technical Summary Report.

2. Generator Test Rig Design - Task 2.2.4.3.2

The generator test rig design was completed during the previous report period, and a description and schematics of the test rig was included in the previous Quarterly Progress Report.

3. Stator Ceramic Seal - Task 2.2.4.3.3

Joints between Metal and Ceramic Components

(a) Materials

The evaluation of brazed joints was continued with the brazing of additional ceramic-columbium specimens. The brazing alloys used during the previous quarter were again employed, and, after evaluation of specimens using both columbium and Cb + 1.0 w/o Zr, the following conclusions were reached:

1. Improved bond strength of brazed alumina bodies was indicated by better wetting of the ceramic when columbium was used during the brazing.

2. An iron-barrier layer coating on columbium can protect the columbium from nickel attack when nickel braze alloys are used.

The results of the specimen tensile tests are presented on Table V.

The following nomenclature is used in Table V:

1. Alumina A is AD-99.5 — Braze X is TiNi (eutectic)

   Alumina B is AL-99.5 — Braze Y is AMS 4778

   Alumina C is Ei-C — Braze Z is NiCu; Washer P is Cb; Washer Q is Cb+ 1 w/o Zr

2. K: indicates 1000 hour exposure of the specimen to potassium at 1100°F before tensile testing.

3. K_G: indicates presence of argon in the capsule with full potassium charge during the 1000 hour exposure at 1100°F.

4. (K): indicates approximately 4.0 grams (20 percent of normal load) of potassium during the 1000 hour exposure.

5. Dates in parentheses are dates for completing full charge, 1000-hour, potassium exposure and subsequent tensile tests.

6. * indicates failure of joint only during 1000-hour potassium exposure.

7. ** indicates failure of ceramic only during 1000-hour potassium exposure.

8. *** indicates failure of the ceramic and the joint during 1000-hour potassium exposure.

9. The unit stress in psi is approximately 5.3 times the fracture load.

TABLE V

TEST RESULTS WITH BRAZED CLM-15 SPECIMENS

Sample	Fracture (Pounds)	Sample	Fracture (Pounds)	Sample	Fracture (Pounds)	Sample	Fracture (Pounds)
AX-1	870	AY-9	390	AZ-19Q	(4/30)K	BZ-1	***K
AX-2	1220	AY-10	550	AZ-20Q	(4/30)K	BZ-2	***K
AX-3	1075	AY-11	(4/30)K			BZ-3	***K
AX-4	870	AY-13	(4/30)K	BX-1	1835	BZ-4	**K
AX-5Q	1060			BX-2	290	BZ-5	1340
AX-6Q	700	AY-14	(4/30)K	BX-3	1220	BZ-6	2550
AX-7P	415	AY-15	(4/30)K	BX-4	860	BZ-7	1450
AX-8P	760	AY-16	(4/30)K	BX-5P	400	BZ-8	1180
AX-9	*K	AY-17Q	(4/30)K	BX-6P	1125	BZ-9	2100
AX-10	470K	AY-18Q	(4/30)K	BX-7Q	1030	BZ-10	2065
AX-11	(low)K	AY-19Q	940	BX-8Q	1375	BZ-11	1290
AX-12	*K	AY-20P	450	BX-9	***K	BZ-12	1800
AX-13P	*K	AY-21P	450	BX-10	**K	BZ-13	1390
AX-14P	30K			BX-11	***K	BZ-14	1400
AX-15P	*K	AZ-1	710(K)	BX-12	***K	BZ-15	2750
AX-16P	*K	AZ-2P	370(K)	BX-13P	***K	BZ-16	540
AX-17P	$702K_G$	AZ-3	100(K)	BX-14P	***K	BZ-17	1270
AX-18P	$152K_G$	AZ-4P	300(K)	BX-15P	***K	BZ-18	2290
AX-19Q	$370K_G$	AZ-5Q	1090(K)	BX-16P	***K	BZ-19	2000
AX-20Q	$268K_G$	AZ-6Q	1225(K)	BX-17Q	(4/30)K	BZ-20	1760
AX-21	*K	AZ-7	260(K)	BX-18Q	(4/30)K	BZ-21	(4/30)K
AX-22	*K	AZ-8	750(K)	BX-19	(4/30)K	BZ-22	(4/30)K
AX-23	*K	AZ-9	(4/30)K	BX-20	(4/50)K	BZ-23	(4/30)K
AX-24P	*K	AZ-10	(4/30)K	BX-21	1020	BZ-24	(4/30)K
		AZ-11	(4/30)K	BX-22	705	BZ-25	(4/30)K
AY-1	1050	AZ-12Q	945	BX-23	910	BZ-26	(4/30)K
AY-2	970	AZ-13Q	1240	BX-24	600	BZ-27	(4/30)K
AY-3	690	AZ-14Q	1690			BZ-28Q	(4/30)K
AY-4	1620	AZ-15Q	1130	BY-1	(4/30)K		
AY-5	1750	AZ-16Q	(4/30)K	BY-2	(4/30)K	CZ-1	(4/30)K
AY-6	1210	AZ-17Q	(4/30)K	BY-3	(4/30)K	CZ-2	(4/30)K
AY-7	1200	AZ-18Q	(4/30)K	BY-4	(4/30)K	CZ-3	(4/30)K
AY-8	700						

(b) Potassium Effects

Tests have indicated that the B grade of alumina (99.5 percent pure) fails during 1000 hours of endurance testing in potassium at 1100°F. The A grade alumina (also 99.5 percent pure) showed a slight surface deterioration; evidence that potassium attack extended at least 50 mils deep was revealed by finding traces of beta-alumina with an X-ray spectroscope. These results, taken from one capsule, indicate that a 10,000 hour life may be questionable. Additional A grade alumina tensile specimens will be sectioned and examined to confirm the potassium attack.

Examination of the brazing alloys after the 1000-hour potassium exposure at 1100°F indicated that all three alloys have good potassium resistance.

The joint failures noted on Table V occurred primarily in the metallized coating zone indicating a need for development of a better metallizing process. The metallizing was performed by commercial methods using molybdenum-manganese.

The cup corrosion specimen samples described in the previous Quarterly Progress Report were not exposed to liquid potassium since it was found to be impractical to produce satisfactory brazes with the required combination of metals in an assembly of this small size.

(c) Helium Permeation

An initial trial of helium permeation was made on a B grade alumina tube; however, an equipment failure prevented completion of the test. Testing will be resumed, and three types of alumina ceramic tubes will be tested.

4. Electrical Insulation - Task 2.2.4.3.4

Testing of the six statorettes described in the last Quarterly Progress Report was continued during this report period. However, encapsulated stator number six was damaged during assembly into the frame, and was removed from the Phase II test program. This statorette has been successfully repaired, and will be tested under Phase III.

Examination of the initial electrical leakage data showed that all three of the alumina sphere filled statorettes displayed a short to ground, or excessive leakage, in at least one location. It is felt that this condition was caused by mechanical damage to the slot liner insulation, resulting from a shifting of the windings during filling with the alumina spheres. The leakage values in the now grounded windings in the sphere-filled statorettes were consistently higher than for the encapsulated statorettes.

Following completion of the thermal cycling and heat aging tests described in the last Quarterly Progress Report, statorettes number 2 (encapsulated) and number 3 (loose alumina sphere filled) were again leakage tested at room temperature, 400°F, 600°F, 800°F, 1000°F, and again at room temperature. The test results indicated that no damage had occurred due to thermal cycling in either statorette, and, in fact, the trend in leakage values after cycling was toward improvement in both units.

There were no detrimental effects in 1004 hours of heat aging at 800°F on the encapsulated statorette. The ceramic enameled conductors in that statorette displayed lower current leakage values after the aging. The loose pellet filled statorette indicated some high current leakage early in the aging process; however, the unit improved throughout the test by showing reduced leakage values. There was no instability or arcing in the final test results.

After the vibration and shock testing of statorettes number 1 (loose alumina sphere filled) and number 5 (encapsulated), it was found that all the glass-served magnetic wire windings of unit number 5 were grounded at 500 volts. However, the ceramic enameled windings performed more satisfactorily. A very high leakage or complete grounding occurred for all windings in the sphere-filled statorette, and it was concluded that vibration had a more severe effect than shock on this unit. The units with rigid encapsulation appear to be more satisfactory than the sphere-filled units due to a greater restraint being exerted on the windings.

5. Generator Rigid Insulation

As reported in the last Quarterly Progress Report, mechanical damage occurred during insertion of wound statorettes into the steel frames and during welding of the coil ends. As a result, no useful test information could be acquired from vibration and shock testing of these units. As a result of this experience, it is concluded that improved tooling and a tighter mechanical design must be developed to preclude destructive shifting of the windings.

6. Joining Hiperco 27 Alloy to Columbium

As reported in the last Quarterly Progress Report, satisfactory joints between Hiperco 27 and columbium can be made by brazing, but cycling, creep, impact and fatigue tests are necessary to evaluate the joining practice properly. The immediate objectives of this task have been met, and the Phase II task is considered complete.

7. 50-KW Liquid Metal Model Generator

The design of the 50-kw liquid metal model generator was completed during the previous quarter, and drawings showing the mechanical layout were included in the last Quarterly Progress Report. The fabrication of the 50-kw generator was initiated during Phase II and is continuing as a part of the Phase III effort.

Several company-funded programs are being conducted by Westinghouse in support of the LMCD II program as follows:

(a) Holwick Pump Development

A test rig has been constructed and a limited number of tests have been run (1) on air with a configuration suitable for use as the generator cavity seal, and (2) on water with a configuration suitable for sealing of the bearing liquid. The test results are very encouraging.

(b) Bearings

A test rig has been constructed and tests performed on water-lubricated bearings simulating the LMCD II application. A back-up program to supply an oil-lubricated bearing configuration has been initiated.

(c) Test Loop

The potassium test loop to be used in testing of the LMCD II has been completed and checked out.

F. Alternate Turbogenerator Design - Task 2.2.4.4

The analysis and design of the alternate turbogenerator is complete; the design is illustrated in Figure 15. The design incorporates a two-bearing arrangement of a six-stage TZM molybdenum alloy (braze assembled) turbine rotor integrally joined to an H-11 alloy axial-gap inductor-generator rotor by means of a curvic coupling. The six-stage configuration was selected on the basis of improved efficiency over the five-stage configuration. However, the initial objectives of the alternate turbogenerator program--the design of a turbogenerator that avoided the use of a ceramic stator seal and the use of generator rotor cooling--were not achieved as feasible alternatives were not devised.

Problem areas anticipated in the development of the alternate turbogenerator design are as follows:

(1) High-temperature operation requires that a stator insulation system be developed that will have both the high temperature and life properties required by SPUR.

(2) Stator windings and insulation cannot at this time be operated in a potassium environment. It is therefore necessary to develop a ceramic seal that can be used to isolate the stator system from the potassium in the generator rotor cavity.

(3) High-temperature mechanical properties of candidate turbine and generator rotor materials must be defined to a sufficient degree of accuracy to permit a sound mechanical rotor design basis to be established.

(4) High-temperature, high-speed liquid metal journal and thrust bearings must be developed before any liquid metal turbogenerator can be considered operable.

These problem areas are presently being investigated in the SPUR program as portions of Air Force Contracts AF33(616)-7379, AF33(616)-8322, and AF33(657)-8954. To date this work has shown that both the ceramic stator seal and the stator insulation problems can be solved.

A summary review of the two turbogenerator designs considered indicates the following:

(1) Turbogenerator unit efficiencies are essentially the same for both units.

(2) The rotor weight of the axial air gap (alternate design) generator is somewhat less than that of the radial air gap machine. The unit weights are, however, the same for both turbogenerator units. Furthermore, since the unit efficiencies are nearly the same, the over-all system weight penalties are the same.

(3) The stress levels in both the turbine rotor and the generator rotor of the axial air gap (alternate design) are somewhat greater than those of the radial air gap machine.

(4) Although the generator rotor in the axial air gap generator is lighter, the bearing loads in the unit are greater because only two bearings are used to support the rotors. The radial air gap machine uses four bearings to support the rotors. In either case, extensive bearing development must continue.

(5) Both units require liquid cooling of both the generator rotor and stator.

(6) Stator seal development programs must be continued for either unit since both units require that the stator regions be protected from the potassium in the rotor cavity.

(7) Both turbogenerator designs require that the stator insulation system development be continued with no advantage seen in one unit over the other with respect to the stator insulation system.

(8) Rotor material mechanical properties investigations must be continued for either design. Since higher stress levels are encountered in the axial air gap machine, the firm definition of these properties, particularly the creep properties, is somewhat more critical for this unit design.

A topical report is now being prepared for this task and, upon completion, will be submitted to the Aeronautical Systems Division for review and approval.

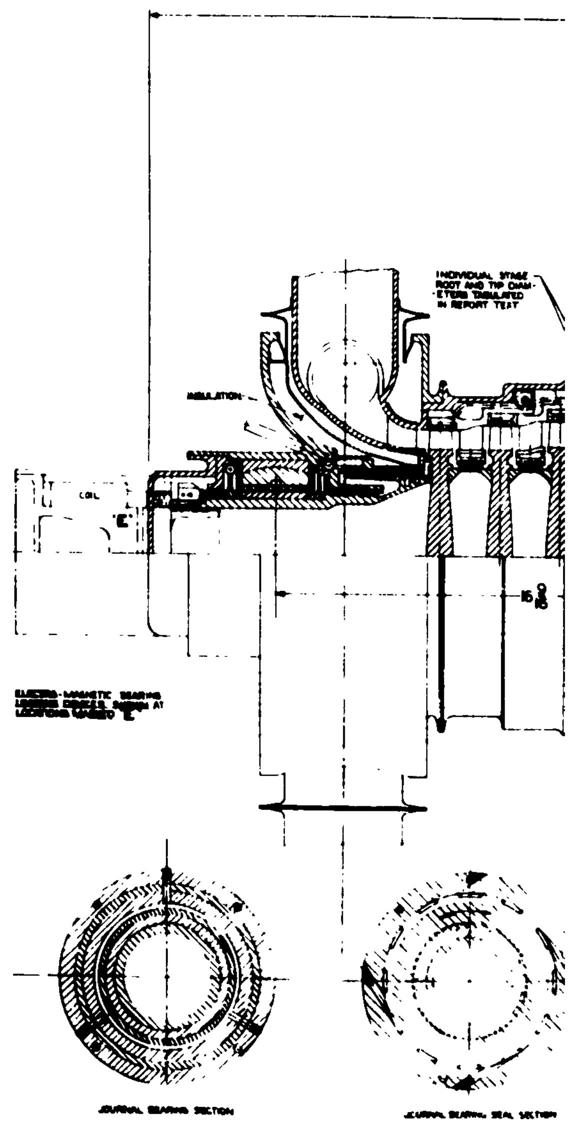
INDIVIDUAL STAGE ROOT AND TIP DIAMETERS TABULATED IN REPORT TEXT
INSULATION
COIL
E
JOURNAL BEARING SECTION
JOURNAL BEARING SEAL SECTION

1

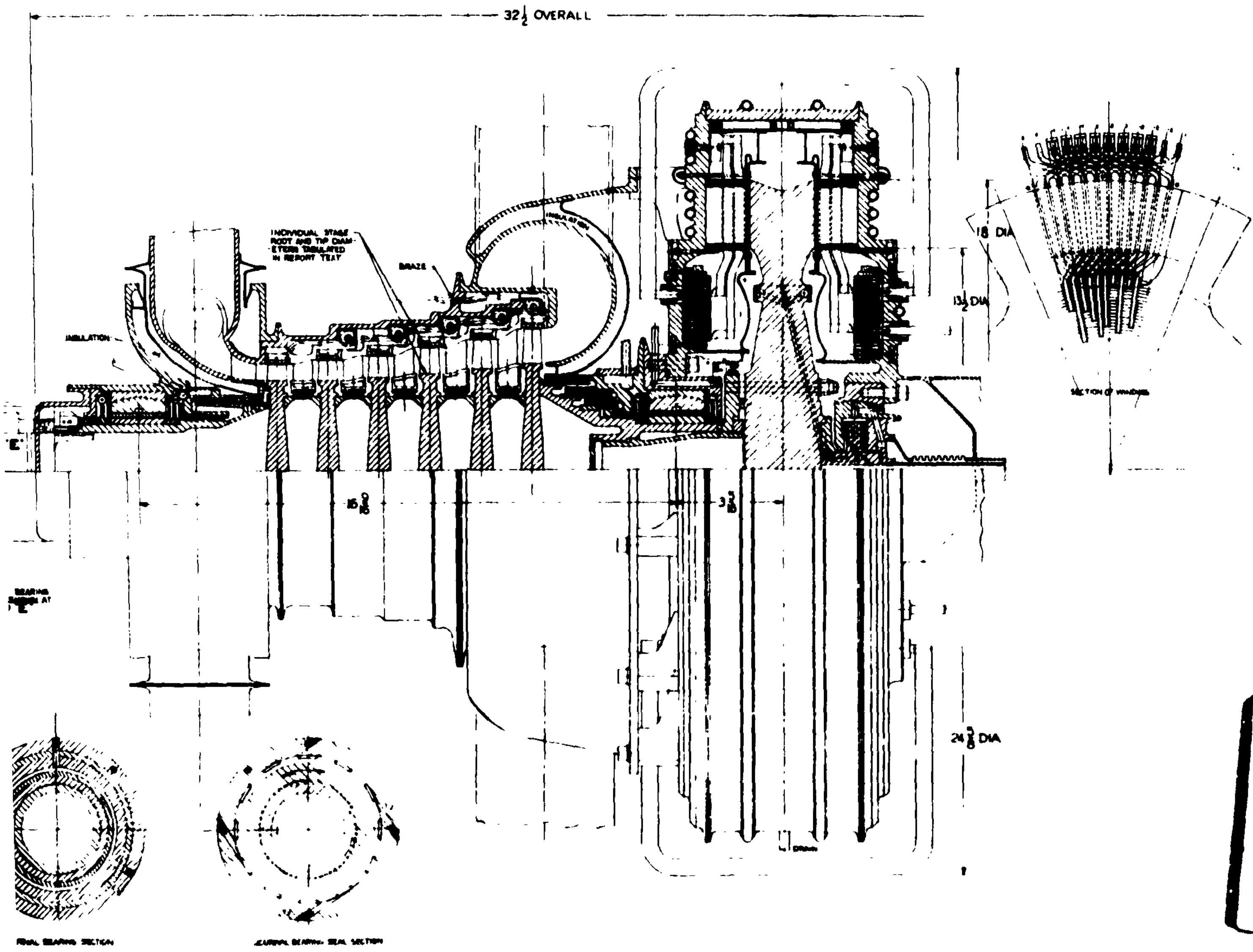

SPUR ALTERNATE TURBOGENERATOR DESIGN

FIGURE 15

G. Heat-Transfer Development

1. Single-Tube Boiling-Potassium Test - Task 2.2.5.1

Assembly of the loop was completed; the instrumentation was installed and the loop was filled. Checkout of the loop operation and the instrumentation was then initiated. The assembled test loop is shown on Figure 16.

2. Vapor-Liquid Separator, Task 2.2.5.2

Assembly of the vapor-liquid separator was completed, and it was installed in the test facility in a horizontal position. Qualitative testing with variations of air flow, water flow, system pressure, and collection gap width indicated a maximum water separation efficiency of about 70 percent over a wide range of air and water flows.

Visual observations indicated that the water would only slightly wet the lucite separator and the water tended to flow in streams from the trailing edges of the turning blades. The resulting nonuniform water film thickness on the tube wall caused difficulty at the collection section. A wetting agent added to the water and a change of water injector nozzles improved the water distribution, but streaming was still evident.

INSTRUMENTATION AND CONTROLS

SINGLE-TUBE BOILING-POTASSIUM
TEST LOOP

FIGURE 16

Observation of the air-water flow patterns at the collection scroll revealed that a portion of the water would enter the collection lip and flow parallel to the lip for a short distance. Then, instead of flowing directly into the scroll, the water was observed to jump the collection lip and proceed back into the main stream. Apparently, an adverse pressure gradient was created by stagnation of the air in the collection scroll. Also, a vortex pattern at the scroll outlet pipe was observed.

A substantial improvement in separator efficiency should be possible if uniform water distribution can be achieved at the collection lip, and if the flow problems in the scroll can be eliminated. These two problems are probably interrelated. Further aerodynamic analyses of conditions at the collection scroll are warranted.

3. Flow Visualization Studies -Task 2.2.5.2

Fabrication of the Freon condenser and boiler was completed, and these units are shown in Figures 17 and 18. The loop design was also completed, and the loop has been fabricated. Testing of this loop will be continued during Phase III.

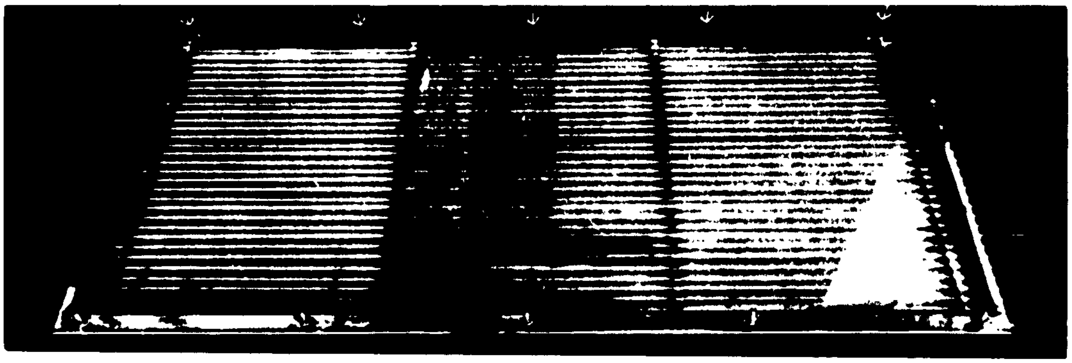

FREON CONDENSER

FIGURE 17

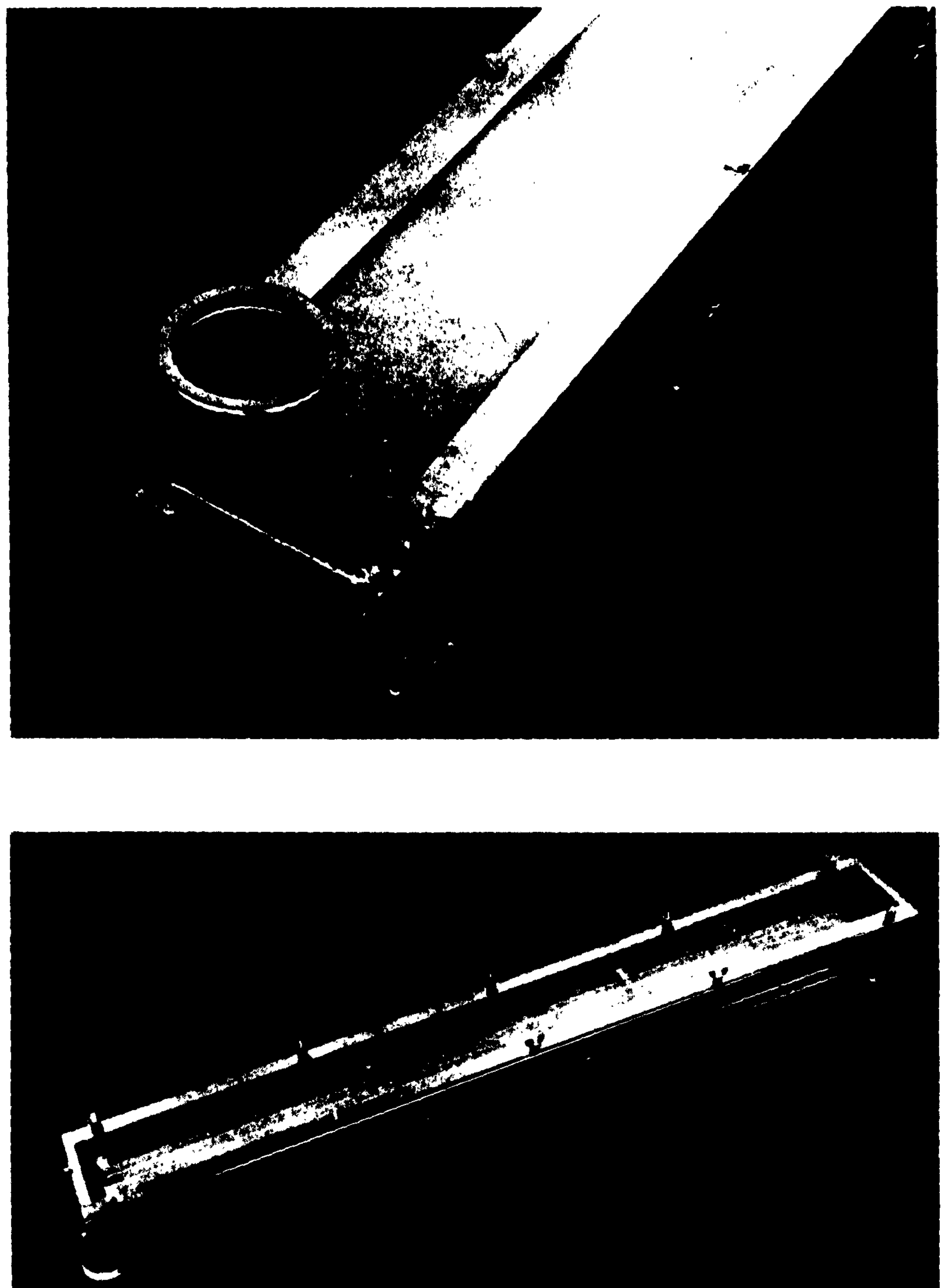

FREON BOILER

FIGURE 18

4. Stainless-Steel Heat-Transfer Components - Task 2.2.5.3

Stress analyses of the recuperator and the separator were performed, and an analysis of the effect of reduced-temperature operation on separator performance was made. Layouts of the recuperator and separator are finished, thus completing the remaining task items. The stainless steel recuperator and separator are shown in Figures 19 and 20, respectively.

5. Stainless Steel Heat-Transfer Loop - Task 2.2.5.4

The test-loop layout has been completed and detailed drawings of the primary and secondary loops are finished. The electrical design and control-system layouts are also completed. Vendors have been selected for major loop components, and the final quotes and delivery schedules on long-lead-time items have been obtained.

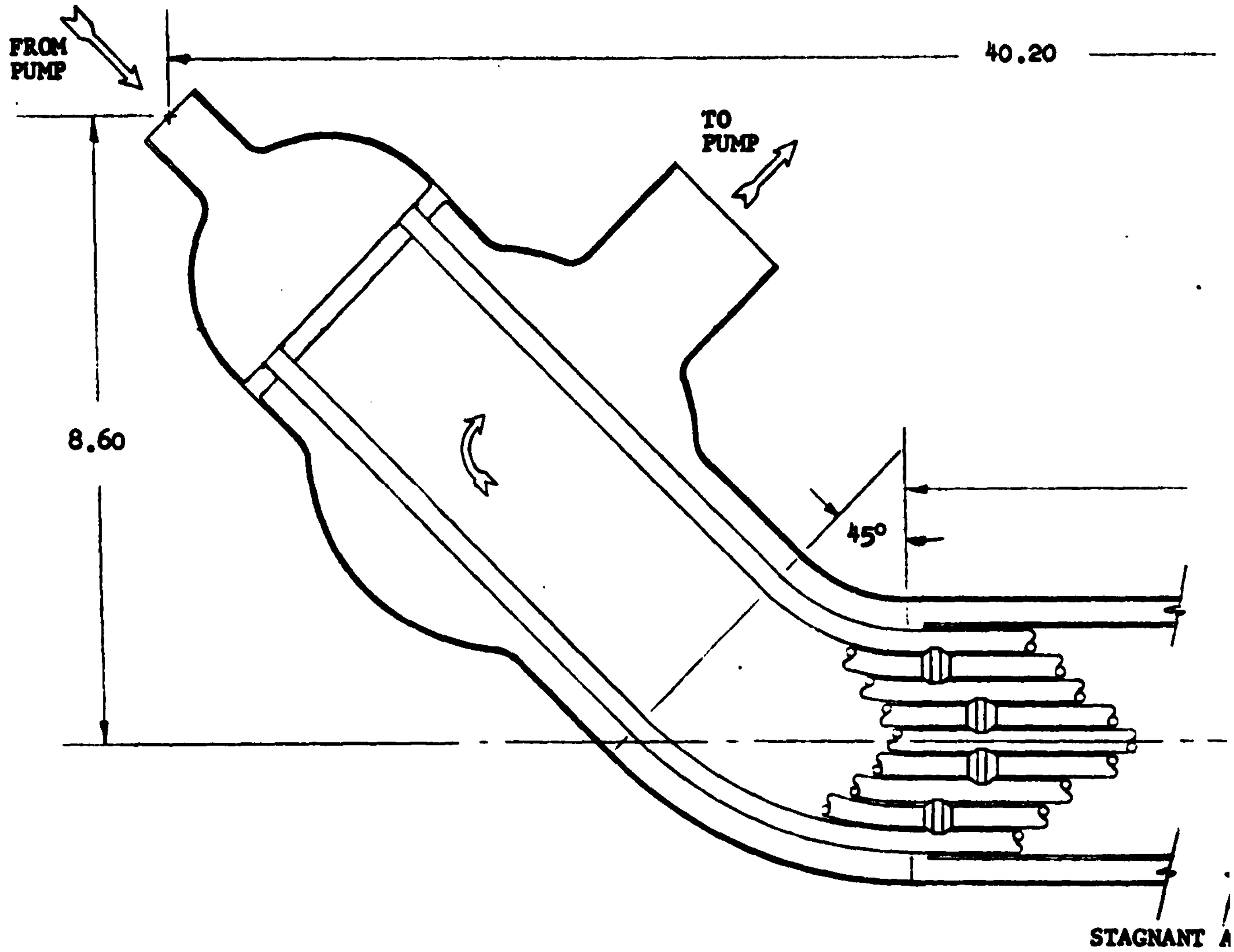

THE GARRETT CORPORATION
AiResearch Manufacturing Division
Phoenix, Arizona

1

FIGURE 19
STAINLESS STEE
RECUPERATOR

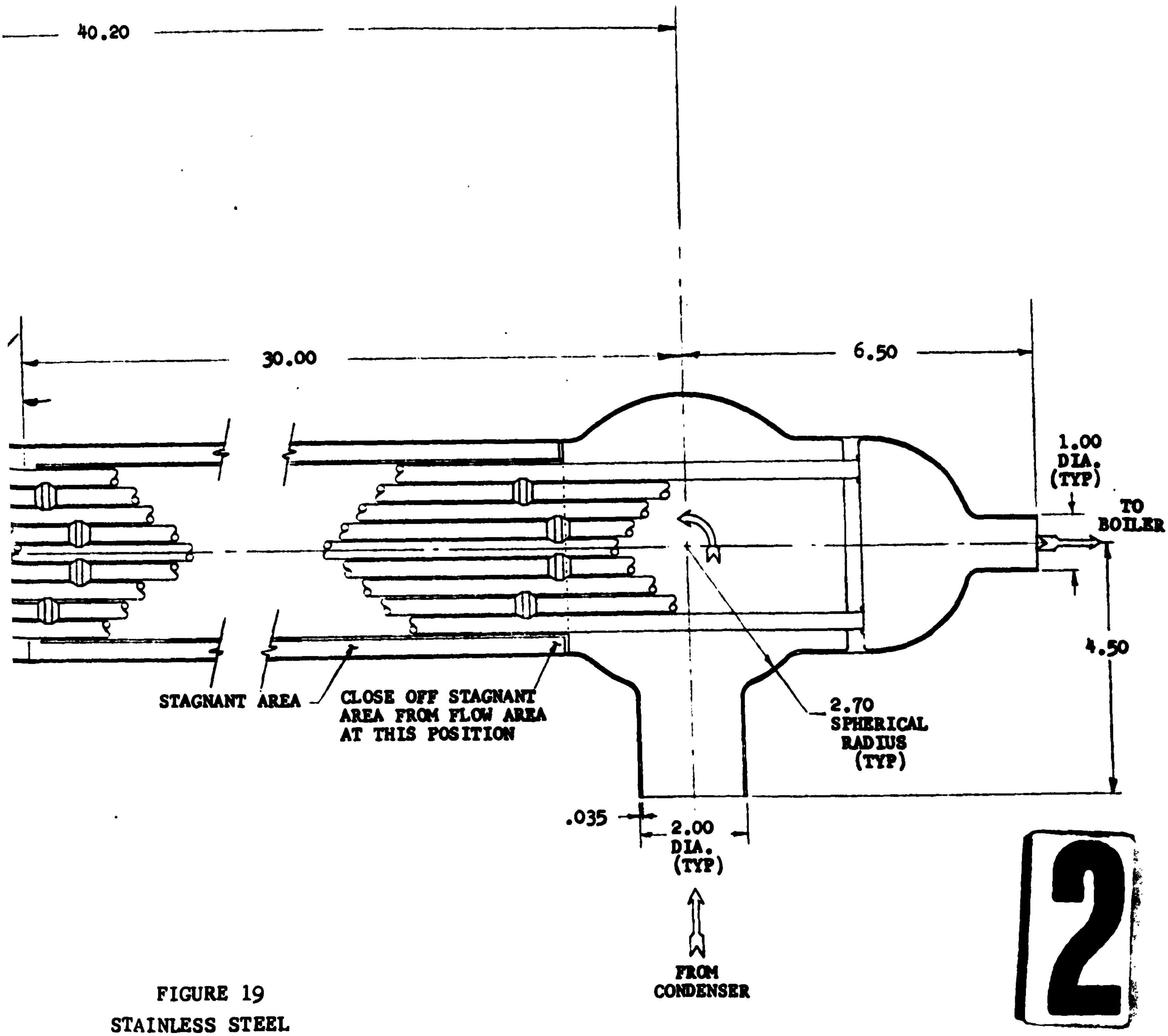

FIGURE 19

STAINLESS STEEL
RECUPERATOR

THE GARRETT CORPORATION
AiResearch Manufacturing Division
Phoenix, Arizona

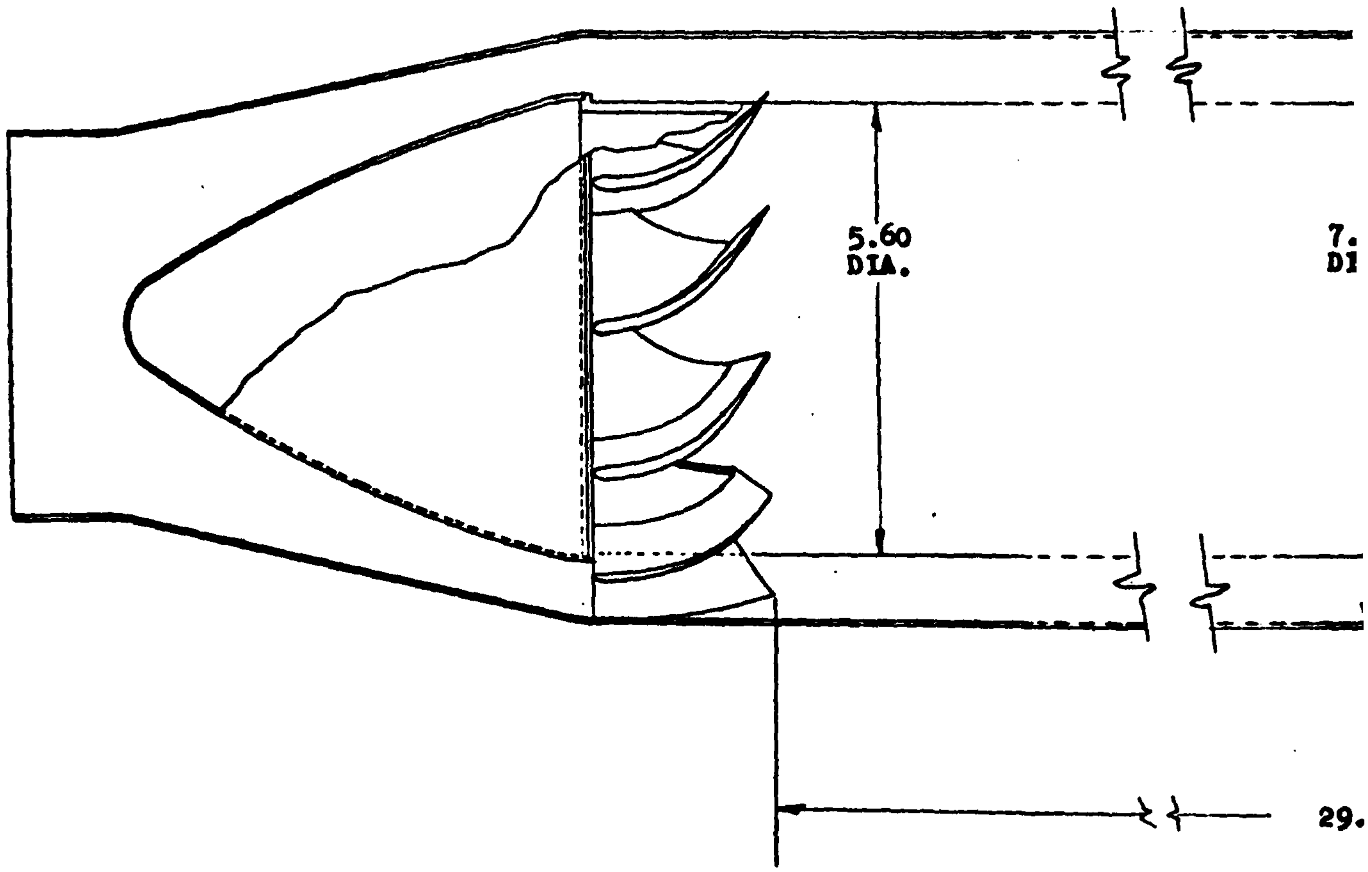

FIGURE 20

STAINLESS STEEL
LIQUID-VAPOR SEPARATOR

1

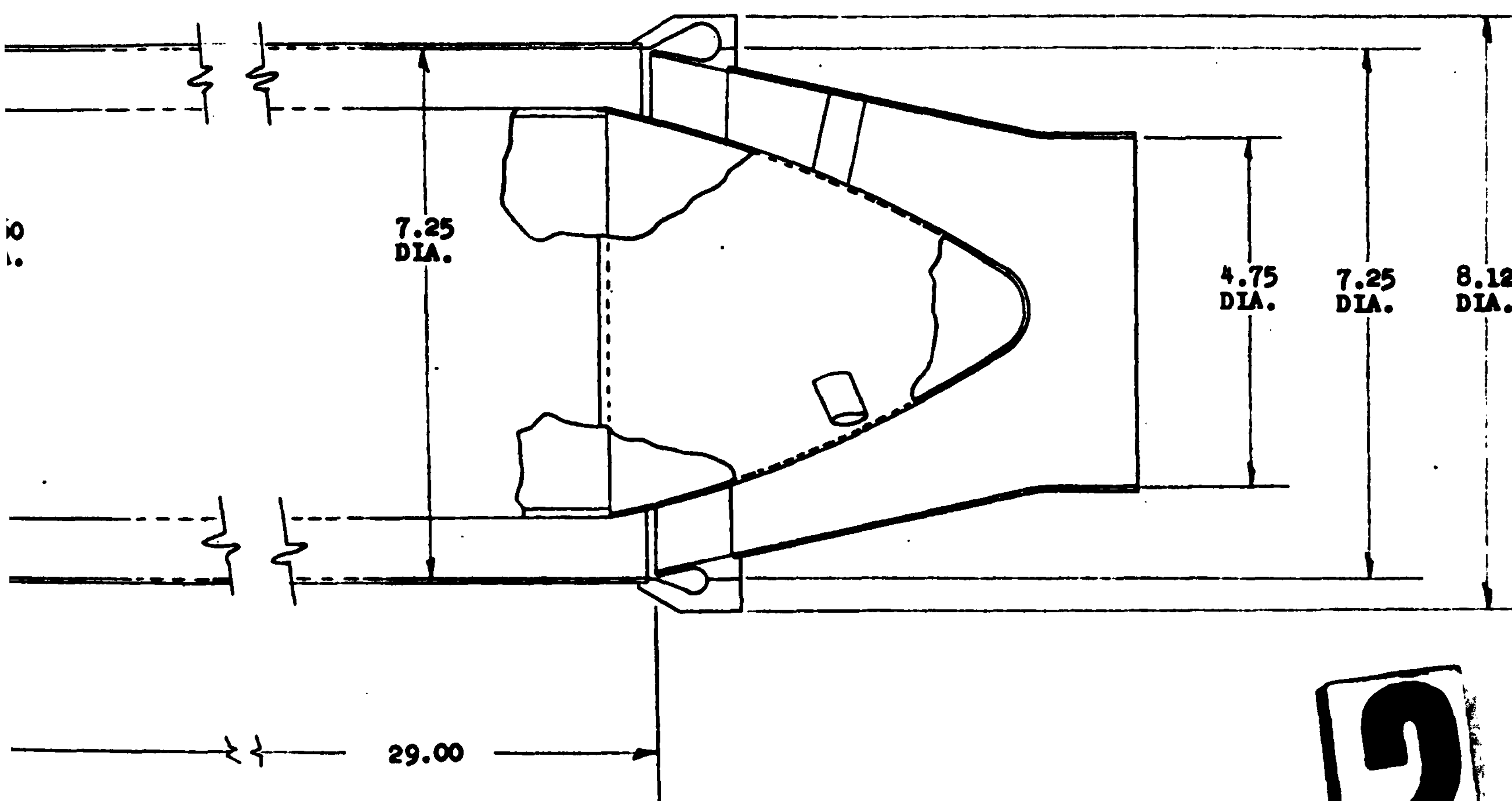

FIGURE 20

STAINLESS STEEL
LIQUID-VAPOR SEPARATOR

H. Controls Development

1. Steady-State Controls Analysis -Task 2.2.6.1

This task was completed during the quarter ending December 31, 1962, as reported in Phase II Annual Technical Summary Report.

2. System Start-Up Analysis - Task 2.2.6.2

This task was completed during the quarter ending December 31, 1962, as reported in the previous Quarterly Progress Report.

3. Controls Experiment - Task 2.2.6.3

This task was completed during the quarter ending December 31, 1962, and a report of the final tests was included in the previous Quarterly Progress Report.

I. Reactor Loop Development

1. Reactor Loop Pump Bearing Test and Loop Simulation - Task 2.3.1.2 and Task 2.3.1.3

Tests of the reactor loop pump and bearing were discontinued and the loop was disassembled for post-test analysis. The analysis indicated:

(a) Some mass transport may have taken place, because of the increased impurity content due to repeated welding and cleaning operations.

(b) The loop failure occurred due to stress corrosion caused by high cyclic stress, presumably vibratory.

(c) Tungsten carbide bearing material (spray-coated on the columbium shaft) apparently reacted with the columbium to form some free tungsten and a columbium-tungsten carbide at the interface between the materials.

(d) No visible pump erosion or corrosion was noted.

The test of the pump bearing system demonstrated the feasibility of lithium-lubricated bearings, as well as demonstrating the application of the centrifugal pump at SPUR reactor loop temperatures.

2. Reactor Loop Controls - Task 2.3.2

This task is complete, as reported in the previous Quarterly Progress Report.

A topical report has been prepared and will be submitted to the Aeronautical Systems Division for review and approval.

3. Properties of Reactor Clad and Structural Materials - Task 2.3.3

Fabrication and installation of the test apparatus has been completed except for (1) the lithium pressure regulators and (2) the tantalum furnace liners.

The furnace liners, although received, did not meet specifications and were returned to the vendor. The regulators were retested after modification by the vendor but still are not able to control the pressure satisfactorily. The vendor now claims that the requirement is beyond the capabilities of the regulators. A study of alternate methods of regulation has been started.

The furnace tests have been initiated, to adjust the controller and furnace gradients to the desired precision. Control stability within ±3°F and an axial gradient varying no more than 3°F over a 10-inch length are desired. Control stability was achieved after the proper thermocouple placement and controller setting was found. Obtaining the uniform furnace gradient has proven to be much more of a problem. The gradient has been improved from 30°F to 6°F maximum variation in tests to date

Work hardening occurred during final machining of the columbium capsules before the final dimensions were achieved.

During the next period, the Cb-1Zr and B-66 capsules will be annealed and finish-machined. The two-stress stainless steel capsule for the trial run will be filled with lithium and Test I will be run. Tests with the refractory capsules will then be run.

The furnace tests have been initiated, to adjust the controller and furnace gradients to the desired precision. Control stability within ±3°F and an axial gradient varying no more than 3°F over a 10-inch length are desired. Control stability was achieved after the proper thermocouple placement and controller setting was found. Obtaining the uniform furnace gradient has proven to be much more of a problem. The gradient has been improved from 30°F to 6°F maximum variation in tests to date.

Work hardening occurred during final machining of the columbium capsules before the final dimensions were achieved.

During the next period, the Cb-1Zr and B-66 capsules will be annealed and finish-machined. The two-stress stainless steel capsule for the trial run will be filled with lithium and Test I will be run. Tests with the refractory capsules will then be run.